12th International Conference on Fracture Mechanics of Concrete and Concrete Structures
FraMCoS-12
B.L.A. Pichler, Ch. Hellmich, P. Preinstorfer (Eds)

https://doi.org/10.21012/FC12.1363
MS01-3:3

FRACTAL PATTERNS FOR FAILURE MODES OF ULTRA-HIGH PERFORMANCE CONCRETE

ZIHAN JIANG, ZHIWEN ZHU

Shantou University, Department of Civil Engineering and Smart Cities
University Road 243, Shantou, 515063, China
E-mail: 19zhjiang@stu.edu.cn

Key words: Fibre-reinforced concrete, Ultra-high performance concrete (UHPC), Size effect, Acoustic emission, Fractal domain

Abstract: From the perspective of fractal theory, the bridging effect of the fibres in ultra-high performance concrete (UHPC), may allow only volume cracks, rather than dominant fractures. Experimental tests are carried out to investigate the emitted energy and the fractal domain of the concrete specimens under compression. UHPC and plain concrete specimens with characteristic size equal to 75, 150, and 300 mm, and slenderness 0.5, 1, and 2, are fabricated. All the specimens are monitored using the acoustic emission (AE) sensors. The results indicate that compression strength and ductility of the block specimens exhibit a strong change by varying the sample size. As size and/or slenderness increase, the structural behaviour exhibits a ductile-to-brittle transition, and the final collapse shows a crushing-to-cracking transition. Moreover, the experimental fractal dimension of plain concrete is closer to 2, demonstrating that the fracture tends to occur on a plane (crack surface, 2-D). In contrast, the fractal dimension of fibre-reinforced concrete is close to 3 due to fibre bridging, which avoids the formation of crack surfaces, being the fractal domain very close to a volume (3-D).

1. Introduction

Size effect describes material strength and ductility as dependent on the characteristic size of the structure. Specifically, small-size specimens show higher apparent strength than large-size samples. In the past years, several size effect laws for concrete have been proposed [1]. Carpinteri's multi-fractal scaling laws (MFSL) is based on the fractal properties of the cracking process, describing the fracture of quasi-brittle materials in a non-integer dimensional space [2]. Additionally, numerical simulations have become a supplementary method for exploring the size effect in cementitious materials [3]. Concerning the size effect of concrete, researchers have done extensive work [4,5]. In particular, acoustic emission (AE) techniques can provide new insights into the concrete size effect on the energy release rate through the fractal theory [6]. Furthermore, according to very recent interpretations [7], the relationship between crack propagation and emitted energy, is represented by the area subtended by each snap-back branch.

This paper presents an experimental investigation of damage using the AE technique. Ultra-high performance concrete (UHPC) and plain concrete specimens with different sizes are tested to investigate the size effect. The emitted energy is experimentally detected during snap-back instabilities of concrete specimens in compression. In particular, the size effect, as well as the total number of AE events, is employed to evaluate the damage domain and its fractal dimension.

2. Testing on UHPC block specimens

2.1 Material properties

The UHPC mix is listed in Table 1. Steel fibres with a length of 12 mm, a diameter of 0.2 mm, and a tensile strength higher than 3000 MPa, are mixed with a fibre volume fraction equal to 2%. UHPC compressive strength is equal to 131.1 MPa after standard curing for 28 days.

Table 1 UHPC mix (kg/m^3)

Component	Cement	Silica ash	Fly ash	Quartz sand	Water	Steel fibre
Dosage	850	137.5	112.5	1100	198	234

Plain concrete used in this study is made using ordinary Portland cement of class 42.5, grade II fly ash, grade S95 slag powder, 5-25 mm crushed gravel, and sand with a fineness modulus of 3.1. The concrete strength grade is C25, and the ratio of cement:sand:stone:water is 1:2.24:2.97:0.48. The compression strength of plain concrete is equal to 33.2 MPa after curing (28 days).

2.2 Specimen geometry

The compression tests are carried out on nine plain concrete specimens (3×3) having characteristic size equal to 75, 150, and 300 mm, and slenderness 0.5, 1, and 2 (Table 2 and Fig.1). The lab equipment used during the testing is illustrated in Fig.2.

Table 2 Specimen geometry

Series	Size (mm)	Slenderness ratio
I	75 × 75 × 37	0.5
	75 × 75 × 75	1
	75 × 75 × 150	2
II	150 × 150 × 75	0.5
	150 × 150 × 150	1
	150 × 150 × 300	2
III	300 × 300 × 150	0.5
	300 × 300 × 300	1
	300 × 300 × 600	2

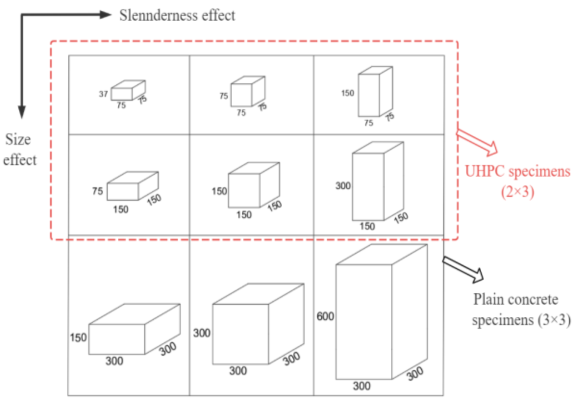

Figure 1 Specimen sizes (mm)

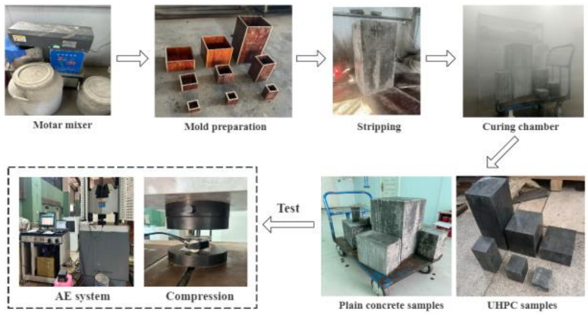

Figure 2 Lab equipment and specimens

2.3 AE monitoring setup

During the axial compression tests, a Teflon sheet is positioned between the platen of the testing machine and the specimen in order to reduce friction and facilitate the transversal deformation. The loading process adopts displacement-control scheme with a constant rate equal to 0.01 mm/s.

The adopted AE system is the ÆMISSION® equipped with piezoelectric sensors working in the range 10kHz-1MHz. Each channel has an independent threshold trigger, automatically extracting AE signals for continuous monitoring. The sensor is glued with silicone resin on the specimen surface as depicted in Fig.3.

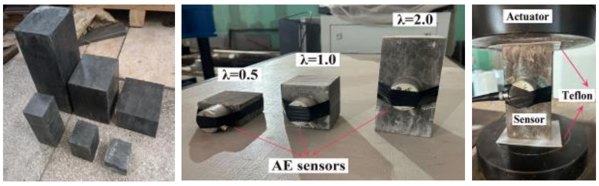

Figure 3 AE sensor layout

3. Experimental results

The experimental results obtained for six UHPC specimens are shown in Fig.4-6. The specimen with slenderness λ = 2 exhibited a global snap-back instability, the post-peak branch being almost vertical compared to that of the stubby specimen (λ = 0.5), which shows a post-peak behaviour characterized by a softening branch (Fig.6). In addition, the related failure mode is governed by a dominant sub-vertical crack, leading the damage evolution up to the final collapse (Fig.4c and 5c).

The load vs. time diagrams of specimens

with λ = 0.5 are characterized by a ductile response in the post-peak stage, also showing a final collapse characterised by compression crushing (Fig.4a and Fig.5a). For high slenderness values, the post-peak curve decreases sharply, and the failure mode is characterised by a single vertical crack (Fig.5c). Thus, a crushing-to-cracking failure mode transition is observed by increasing the specimen slenderness, together with a decrease in the compression strength (Fig.6).

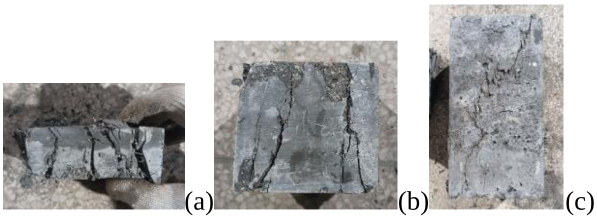

Figure 4 Failure modes of UHPC specimens with size equal to 75 mm and different slenderness ratios: (a) λ = 0.5; (b) λ = 1; (c) λ = 2

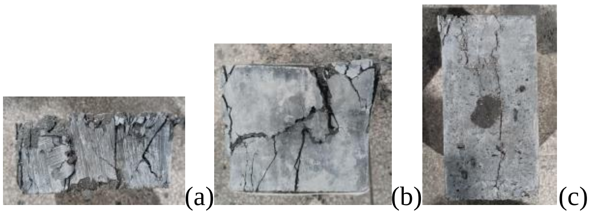

Figure 5 Failure modes of UHPC specimens with size equal to 150 mm and different slenderness ratios: (a) λ = 0.5; (b) λ = 1; (c) λ = 2

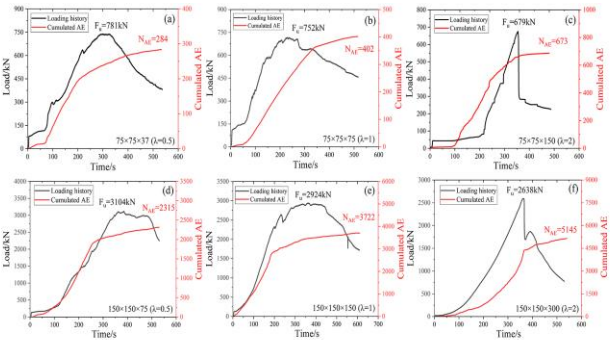

Figure 6 AE monitoring of UHPC specimens

4. Fractal patterns

The energy detected during microcrack propagation, E, is emitted over a fractal domain comprised between a surface and a volume [8]. Therefore, the following size-scaling law is assumed for the energy emission during fragmentation:

$$E \propto V^{D/3} \tag{1}$$

where the fractal exponent, D, is comprised between 2.0 and 3.0 [6]. Considering L as the characteristic size of the specimen, clearly $V^{D/3} = L^{D}$. This indicates that the fractal energy density, i.e.,

$$\Gamma = \frac{E}{V^{D/3}} \tag{2}$$

can be considered as a size-independent parameter [9].

Furthermore, AE can be detected during microcrack propagation. The energy emission, E, is proportional to the total number of AE events $N_{\max}$ [9]. Accordingly:

$$\Gamma_{AE} = \frac{N_{\max}}{V^{D/3}} \tag{3}$$

where Γ_{AE} is the AE signal fractal density [10].

The total number of AE events and loading history from UHPC and plain concrete specimens are shown in Fig.6 and Fig.7, where a strong correlation between AE bursts and snap-back phenomena can be detected. In Fig.8, $N_{\max}$ is represented as a function of the specimen volume, fitting the experimental data. For plain concrete specimens (Fig.8b), the slope in the log-log plane equal to 0.73, i.e. a fractal dimension equal to 2.19, emphasizes that the energy emission occurs in a fractal domain close to a plane (crack surface, 2-D). For fibre-reinforced concrete (UHPC) specimens (Fig.8a), a slope in the log-log plane equal to 0.92 is found, i.e. the fractal dimension is equal to 2.76, the fracture occurring in a domain close to a volume (3-D) due to the higher ductility given by the fibre-reinforcements to the concrete matrix [11-13].

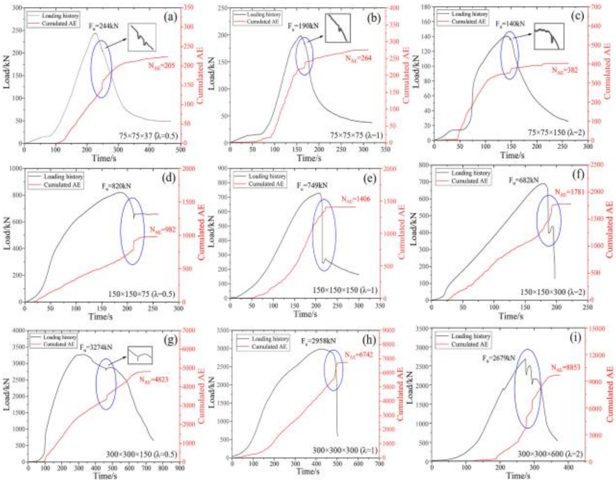

Figure 7 AE monitoring of plain concrete specimens

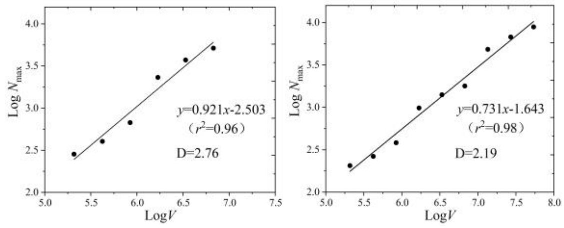

(a) UHPC (b) Plain concrete

Figure 8 Size-slenderness scale in damage evolution.

5. Conclusions

This paper investigates the size effects on failure mode of UHPC and plain concrete block specimens, to verify the beneficial contribution due to the bridging action of fibre-reinforcements. The conclusions are as follows.

(1) As the specimen size increases, its compression strength decreases, and the fracture behaviour exhibits a ductile-to-brittle transition. In addition, as the specimen slenderness increases, the final collapse shows a crushing-to-cracking failure transition.

(2) The energy emission occurs in a fractal domain comprised between a volume and a surface. The experimentally determined fractal dimension of the dissipated energy in plain concrete is closer to 2 (D=2.19), emphasizing that the fracture tends to occur on a plane (crack surface, 2-D). On the contrary, the experimentally determined fractal dimension of the dissipated energy in UHPC is closer to that of a volume (D=2.76) due to the fibre bridging action, which avoids the formation of dominant cracks.

References

[1] Carpinteri A, Chiaia B, Ferro G. Structures, size effects on nominal tensile strength of concrete structures: multifractality of material ligaments and dimensional transition from order to disorder. Mater Struct 1995;28(6):311–317.

[2] Carpinteri A, Chiaia B. Multifractal scaling laws in the breaking behaviour of disordered materials. Chaos, Solit and Fractals 1997;8(2):135–150.

[3] Sinaie S. Application of the discrete element method for the simulation of size effects in concrete samples. Int J Solids Struct 2017;108:244–253.

[4] Muciaccia G, Rosati G, Luzio GD. Compressive failure and size effect in plain concrete cylindrical specimens. Constr Build Mater 2017;137:185–94.

[5] Chen P, Liu CY, Wang YY. Size effect on peak axial strain and stress-strain behaviour of concrete subjected to axial compression. Constr Build Mater 2018;188:645–55.

[6] Carpinteri A, Lacidogna G, Pugno N. Structural damage diagnosis and life-time assessment by acoustic emission monitoring. Engng Fract Mech 2007;74:273–289.

[7] Carpinteri A, Accornero F. Multiple snap-back instabilities in progressive microcracking coalescence. Engng Fract Mech 2018;187:272–281.

[8] Carpinteri A, Corrado M, Lacidogna G. Three different approaches for damage domain characterization in disordered materials: fractal energy density, b-value statistics, renormalization group theory. Mech Mater 2012;53:15–28.

[9] Lacidogna G, Accornero F, Carpinteri A. Influence of snap-back instabilities on Acoustic Emission damage monitoring. Engng Fract Mech 2019;210:3-12.

[10]Carpinteri A, Lacidogna G, Accornero F, Mpalaskas A, Matikas T, Aggelis D. Influence of damage on the acoustic emission parameters. Cem Concr Compos 2013;44:9–16.

[11]Jiang Z, Zhu Z, Accornero F. Tensile-to-shear crack transition in the compression failure of steel-fibre reinforced concrete: Insights from AE monitoring, Buildings 2024; 14:2039.

[12]Accornero F, Rubino A, Marano G, Carpinteri A. Smart construction of fibre-reinforced concrete structures: Size-scale effects on minimum reinforcement and plastic rotation capacity, Smart Construction and Sustainable Cities 2024; 2:12.

[13]Carpinteri A, Accornero F, Rubino A. Scale effects in the post-cracking behaviour of fibre-reinforced concrete beams, International Journal of Fracture 2023; 240(1):1-16.